# Determination of the Plastic Work Converted to Heat Using Radiometry

by D. Macdougall

ABSTRACT—An improved calibration method for infrared radiometers is developed that has been shown to increase the accuracy of temperature measurement. To validate this new calibration technique, high strain rate compression tests are performed on the aluminum alloy BS 2011 and high strain rate torsion tests are performed on the titanium alloy 90%Ti-6%Al-4%V. The adiabatic temperature rise that occurs during these tests is measured using an infrared radiometer and validated, in the case of the compression tests, using fast response thermocouples. The proportion of plastic work converted to heat, β, is found to increase with plastic strain for both materials, which is similar to previous research. These results challenge the classical assumption that β has a constant value of approximately 0.95.

KEY WORDS—Radiometry, plastic work, constitutive models, high strain rate

The conversion rate of plastic work to heat, β, is an important quantity. It is necessary in finite element simulations involving plasticity where temperature calculations are made. Accurate knowledge of β is especially important in finite element simulations of impact events where adiabatic heating may occur, resulting in large temperature rises.

To make measurements of β during high strain rate split Hopkinson bar tests, a rapid temperature measurement technique such as infrared radiometry is required. Radiometry is well suited for this purpose because it is noncontact, has a typical response time of $\sim 1\mu s$ and with a suitable detector can measure temperatures accurately above 30°C. Infrared radiometry has been used on several occasions to measure specimen surface temperature during high strain rate material tests.[1–12]

For the purpose of calculating values of β, measurements of the nominally uniform temperature field that exists early in split Hopkinson pressure bar tests must be made. Measurements using single-element detectors have been made in split Hopkinson pressure bar tests in high strain rate compression,[6,8] tension[5,7,13] and torsion.[2–4]

Historically, β was generally assumed to be a constant in the region of 0.85 to 0.95 for metals. In contrast to this assumption, some researchers[5–8,11,16] have reported values that are lower than the classical region and also vary with plastic strain. A summary of published data of measurements of β for a number of materials is shown in Table 1. Two values of β are quoted for most of the references, representing the range of instantaneous values of β as it varies from low to high plastic strain and the average value of β across the entire test. A majority of these data have been obtained using infrared radiometry, but thermocouples and calorimetry have also been used as indicated in Table 1. These alternative techniques are usually not favored because they are too slow to follow the specimen temperature during an impact test, instead producing a single average value. However, very small thermocouples embedded in a polymeric specimen have been used to follow the temperature history of a compression test.[14,21] This was made possible by casting the polymer around the thermocouple or back-filling the thermocouple hole with the same material as the test specimen.

Table 1 shows that most of the low values of β that have been reported also show variations of β with plastic strain. Often, the value of β is low initially and increases with plastic strain,[1,5,7,8,13,15,16] although more complex variations have been reported.[6]

This wide range of results for β on similar materials has raised some doubt over the validity of the radiometric method. Kapoor[8] carried out compression tests on several materials using radiometry. He also carried out interrupted tests on identical specimens that were then heated to the temperature measured in the continuous test and reloaded. The flow stress measured in the reloaded interrupted specimen was above that measured in a continuous test. This suggests that the actual temperature of the continuously tested specimen was higher than that measured using the radiometer. Kapoor concluded that this error in measurement was due to a problem with the calibration method used for the radiometer.

The calibration of radiometers is usually carried out with the specimen being placed between the loading bars prior to the test, in order to recreate the conditions of the test as closely as possible. The specimen is heated either in an oven before being placed in position or in situ using a soldering iron or hot air gun. Kapoor suggested that the error in the calibration method is connected to the difference in duration of the calibration, which may be several minutes, and the test, often less than 1 ms. In the calibration, the surrounding air and apparatus are heated by the hot specimen, but in the test they remain at room temperature.

In this work, a new calibration method is presented in which the specimen is heated in a specially designed rig that removes spurious sources of radiation. High strain rate compression tests were performed on an aluminum alloy with the temperature rise being measured using the newly calibrated

*D. Macdougall, Department of Engineering Science, Oxford University, Oxford, OX1 3PJ United Kingdom.*

*Original manuscript submitted: May 28, 1999.*
*Final manuscript received: April 25, 2000.*

TABLE 1—PREVIOUS MEASUREMENTS OF THE PROPORTION OF WORK CONVERTED TO HEAT, β

| Material | Test | Strain Rate | Maximum ε | β Value Range $\varepsilon_{low} - \varepsilon_{high}$ | β Mean | References |
|---|---|---|---|---|---|---|
| Steel (4340) | comp. (R) | 3000 $s^{-1}$ | 0.20 | 0.4 – 0.9 | 0.75 | Mason[6] |
| Steel (mild) | torsion (R) | 0.003 $s^{-1}$ | 1.2 | 0.87 – 0.93 | 0.90 | Taylor[15] |
| Steel (224) | comp. (T) | 4 $s^{-1}$ | 0.36 | 0.95 | 0.95 | Dixon[17] |
| Steel (1018) | comp. (R) | 3000 $s^{-1}$ | 0.56 | | 0.80 | Kapoor[8] |
| Cu | torsion (C) | 0.003 $s^{-1}$ | 2.6 | 0.89 – 0.95 | 0.92 | Taylor[15] |
| Cu | comp. (R) | 3000 $s^{-1}$ | 0.90 | | 0.75 | Kapoor[8] |
| Cu | tension (R) | 1700 $s^{-1}$ | 0.34 | 0.6 – 0.8 | 0.75 | Hayashi[5] |
| Ti6A14V | torsion (R) | 460 $s^{-1}$ | 0.22 | 0.2 – 0.7 | 0.45 | Macdougall[11] |
| | | 700 $s^{-1}$ | 0.22 | 0.12 – 0.35 | 0.25 | Macdougall[11] |
| Ti6A14V | comp. (R) | 3000 $s^{-1}$ | 0.18 | 1.0 – 0.5 | 0.80 | Mason[6] |
| Ti (pure) | comp. (R) | 3000 $s^{-1}$ | 0.45 | | 0.60 | Kapoor[8] |
| Ti (pure) | comp. (R) | 1 $s^{-1}$ | 0.36 | 0.60 – 0.70 | 0.65 | Hodowany[16] |
| | | 3000 $s^{-1}$ | 0.45 | 0.75 – 1.0 | 0.88 | Hodowany[16] |
| Al (6061) | comp. (R) | 3000 $s^{-1}$ | 0.72 | | 0.85 | Kapoor[8] |
| Al | tension (R) | $2500^{-1}$ | 0.50 | 0.90 | 0.90 | Hayashi[5] |
| Al (2024) | comp. (R) | 3000 $s^{-1}$ | 0.33 | (0.5) – 0.9 | 0.80 | Mason[6] |
| Al (2024) | comp. (R) | 1 $s^{-1}$, 3000 $s^{-1}$ | 0.53 | 0.3 – 1.0 | 0.60 | Hodowany[16] |
| Al (LY12) | tension (R) | 400 $s^{-1}$ | 0.19 | 0.25 – 0.55 | 0.35 | Xia[7] |
| Al (2017) | tension (R) | 1400 $s^{-1}$ | 0.27 | 0.5 – 0.8 | 0.70 | Hayashi[5] |
| Ta-W alloy | comp. (R) | 3000 $s^{-1}$ | 0.30 | 0.4 – 0.8 | 0.68 | Kapoor[8] |
| Epoxy resin | comp. (R) | 2500 $s^{-1}$ | 0.65 | 0.0 – 0.25 | 0.1 | Trojanowski[12] |
| Polycarbonate | comp. (R) | 8500 $s^{-1}$ | 0.63 | 0.0 – 1.0 | 0.6 | Rittel[14] |
| Polycarbonate | comp. (R) | 5000 $s^{-1}$ | 0.43 | 0.0 – 0.4 | 0.2 | Rittel[14] |

R = radiometry; T = thermocouple; C = calorimetry

radiometer. To validate these results, similar tests were carried out with small thermocouples embedded in the surface of the specimens. Also, radiometric results from high strain rate torsion tests presented previously[1,3] were recalibrated using the new method.

## Existing Theories for Variations of β

Until recently, the proportion of plastic work converted to heat, β, has been assumed to be a constant, usually in the range of 0.85 to 0.95. However, experimental evidence that challenges this assumption has been reported (see Table 1). In addition, theoretical studies have been carried out to explain these experimental results.

### *Zehnder Model*

Zehnder[18] proposed a model for the variation of β with plastic strain. This model is based on the assumption that strain hardening is caused by dislocation multiplication. Zehnder examined the energy of a dislocation and assumed a production rate proportional to the rate of increase of the stored energy of cold work. This produces a model for β that is a function of the strain-hardening coefficient:

$$\beta = \frac{n\left(\frac{\varepsilon_p}{\varepsilon_0}\right)^{\frac{n-1}{n}} - 1}{\left(\frac{\varepsilon_p}{\varepsilon_0}\right)^{\frac{n-1}{n}}}, \tag{1}$$

where $n$ is the strain-hardening coefficient, that is, $\sigma = \sigma_0 + A.\varepsilon_p^{(1/n)}$; $\sigma_0$ and $\varepsilon_0$ are the stress and strain at yield, respectively; and $\varepsilon_p$ is the plastic strain.

This model predicts that materials will start with a low value of β that will increase at higher plastic strain. Materials that demonstrate low strain hardening will therefore exhibit high values of β. Also, the worked state of a material is likely to exhibit a higher value of β than the annealed state. This model can also predict a strain rate sensitivity for β for materials that show a strain rate sensitivity of their strain-hardening coefficient. This behavior is present in some face-centered-cubic metals.

Experimental evidence exists that supports this model's prediction that β increases with plastic strain for aluminum alloys,[5,6,16] copper,[5] steel,[6] titanium[16] and a tantalum-tungsten alloy.[8]

### *Rosakis Model*

A more sophisticated study of the variation of β was carried out by Rosakis.[19] This work concluded that the stored energy of cold work, $E(\varepsilon_p)$, is a function of an internal variable assumed to be strain. The heating rate is defined as the plastic work rate minus the rate of stored energy of cold work,

$$\dot{Q}_p = \dot{W}_p - \dot{E}, \tag{2}$$

which can be written

$$\rho \cdot c \cdot \dot{\theta} = \sigma(\varepsilon, \dot{\varepsilon}_p, T) \cdot \dot{\varepsilon}_p - \frac{dE(\varepsilon_p)}{d\varepsilon_p} \cdot \dot{\varepsilon}_p. \tag{3}$$

By integrating this expression, $E(\varepsilon_p)$ can be calculated from experiments at any strain rate by measuring the mechanical response and the adiabatic temperature rise using

$$E(\varepsilon_p) = \int_0^{\varepsilon_p} \sigma(\varepsilon_p, \dot{\varepsilon}_p, T) d\varepsilon_p - \rho \cdot c \cdot \theta(\varepsilon_p, \dot{\varepsilon}_p). \quad (4)$$

Using eqs (2) and (3), the proportion of work converted to heat is therefore

$$\beta = \frac{\dot{Q}_p}{\dot{W}_p} = 1 - \frac{\frac{dE(\varepsilon_p)}{d\varepsilon_p}}{\sigma(\varepsilon_p, \dot{\varepsilon}_p, T)}. \quad (5)$$

Using this expression and a measure of $E(\varepsilon_p)$ from (4), it is possible to predict the variation of $\beta$ with strain, strain rate and temperature if the constitutive relation is known for the material. Also, materials that show considerable strain hardening or strain rate hardening will have corresponding variations for $\beta$ with either strain or strain rate, respectively.

This model has been shown experimentally to predict the variation in the proportion of work converted to heat with strain and strain rate.[20] This suggests that the assumption is correct that the stored energy of cold work is a function of strain alone, and independent of strain rate.

These models challenge conventional assumptions by postulating that $\beta$ is history dependent and therefore must not be assumed to be a constant.

## Infrared Radiometry

The radiometer used in this work has been described previously,[4] so details of its design will not be shown here. However, significant improvements have been made to the calibration technique employed for the radiometer and are described in this section.

The most critical part of the radiometry technique is the calibration method used. The calibration produces a relationship between the radiometer output and the surface temperature of the specimen. This calibration function will depend on the surface condition of the specimen and may change during the test.

The detector is susceptible to considerable low-frequency noise. For this reason, electronics are used to filter out frequencies below ~ 10 Hz, which have no effect on the high-speed test. As a result of this, the radiometer is unable to record constant or slowly changing signals. In the calibration, an optical chopper disk is required to produce a pseudo-AC signal. A typical signal from the calibration has been presented.[4] The radiometer signal is taken as the peak-to-peak measurement that represents the difference in radiation between the specimen and the chopper disk.

### *Sources of Error in the Calibration Process*

The main potential error in the calibration is from radiation that is not present in the high-speed test. There are two sources for this radiation. First, the air in front of the test specimen becomes heated by the specimen during the calibration. The air is not heated significantly during the high-speed test. Air emits radiation within the wavelength band to which the infrared detector is sensitive (2.0μm to 12.7μm). These emissions are caused by molecular transitions in quantum states of vibration, rotation and translation or by electronic de-excitation. To quantify this source of error, a calculation was made of the power radiated by the air in front of the specimen. Theoretical calculations of molecular emission intensities are very complex, so Modtran version 3.7,[20] which has a database of molecular spectra with which the expected emissions from the atmosphere can be integrated, was used.

The air that emits radiation into the optics is a conic section, and the air temperature, although unknown, is likely to fall off quite rapidly with distance from the specimen surface. Without such data and because of software limitations, a worst-case approximation was used for the calculation. The emissions from a 1 cm × 1 cm × 1 cm cube of air were calculated for temperatures of 20°C and 100°C and were scaled to compensate for the solid angle of the optics. The power that would fall onto the detector from this cube varies between 0.2 nW at 20°C and 0.8 nW at 100°C. This can be compared with the power that would strike the detector emitted by the 1 mm × 1 mm square on the surface of the specimen, which varies between 12μW at 20°C and 32μW at 100°C. This demonstrates that the error caused by the effect of heating the air in the calibration is less than 0.002 percent.

The second source of unwanted radiation is the surrounding apparatus. These objects may also be present in the test, but because they are constant sources of radiation they have no effect. In the calibration, the chopper wheel may make these otherwise constant signals visible to the radiometer. More seriously, objects near the specimen, such as the loading bars, may become heated during the calibration. These will emit radiation onto the surface of the specimen, some of which may be reflected into the optical system. The new calibration rig described in the next section aims to minimize these sources of error.

### *New Calibration Rig Design*

To remove unwanted sources of radiation to make an accurate measure of the signal from the specimen, the calibration could no longer be carried out with the specimen in situ. Instead, the specimen was placed in a specially designed rig, in the same position relative to the radiometer as in the test. A schematic diagram of the new calibration rig is shown in Fig. 1.

The front end of the radiometer comprises an optical system with a cylindrical housing. The calibration rig was mounted onto the front of this housing so that the specimen was positioned automatically. The specimen was surrounded by a copper block to ensure a uniform temperature. A removable section allowed access to insert and remove the specimen. The block was heated with two electric elements and could be raised to a temperature of more than 90°C. A thermocouple was positioned inside the copper block, just behind the specimen, to monitor the temperature.

It was necessary to prevent unwanted radiation from the copper block entering the optical system. This was achieved using a copper disk with a 3 mm diameter aperture, water cooled to ~ 12°C. This disk was mounted on an insulating layer of Tufnol, which was attached to the hot copper block. The disk was ~ 0.2 mm thick and positioned ~ 0.5 mm in front of the specimen surface. The inside surfaces were sprayed with a fine layer of matte black paint to absorb any reflected radiation.

The radiometer signal during the calibration was measured as the peak-to-peak voltage of the chopped signal. This signal represents the difference between the radiation received from the specimen and that received from the chopper disk. If the

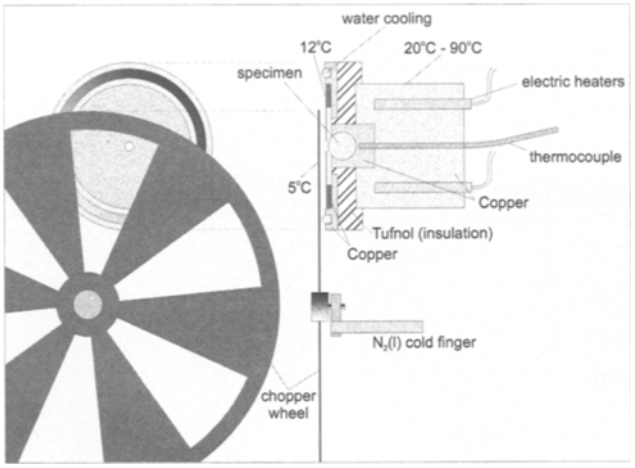


Fig. 1—Schematic of the calibration rig

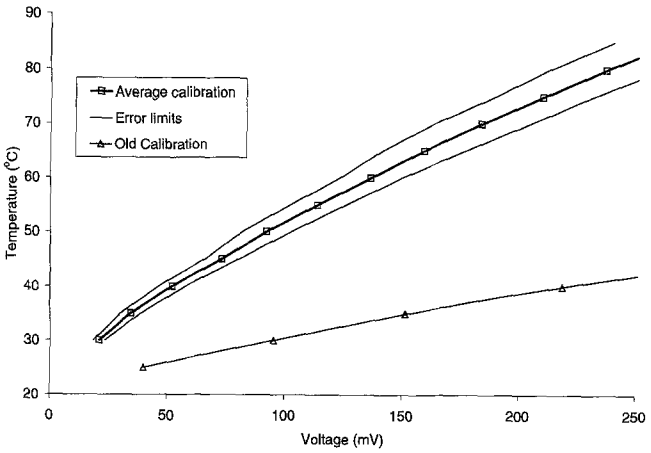


Fig. 2—Calibration of the radiometer with error bounds compared to the old calibration [4]

chopper disk becomes heated, the signal will therefore be reduced. For this reason, a "cold finger" was used to chill the chopper disk to $\leq$ 5°C. This comprised a copper rod linking the axle of the chopper wheel with a flask of liquid nitrogen. The chopper disk was also sprayed black to reduce any unwanted reflections. The heat transfer from the chopper disk through the axle was quite poor, and the temperature of the disk took several minutes to equilibrate.

Previous calibrations have used the same specimen in both the calibration and the test. This was not possible in this case because the specimen was damaged slightly on removal from the calibration rig. Instead, several calibrations were performed on nominally identical specimens, with the same surface condition, to obtain the spread of the calibration. This is likely to introduce a small error into the method.

As in a previous paper,[4] a thin layer of soot was applied to the test specimens to increase the emissivity. Figure 2 shows the calibration for the radiometer with the sooted compression specimens. An upper limit and a lower limit that represent the estimated error are shown that correspond to an uncertainty that increases with temperature from ±2°C to ±4°C. Also shown in Fig. 2 is the calibration curve produced using the old calibration method.[4] This demonstrates the considerable change in calibration produced using the new method.

### *Radiometry Testing Technique*

The radiometry testing technique was very similar to that described previously.[4] The setup and alignment techniques were identical to the previous method, in which a fine steel pointer was attached to the front of the optics in the position of the focus point. This was used as a guide to position the rig in front of a dummy specimen placed between the loading bars.

The positioning of the radiometer relative to the test specimen is dependent on the loading technique. In the torsion test, the specimen ends rotate but the center of the specimen does not translate. Therefore, the alignment position is the center of the specimen. In the compression test, the entire loading assembly and specimen translate. The radiometer must therefore be aligned slightly off-center, so the specimen remains in view during the test. The specimen temperature is measured just prior to the test using a thermocouple. This provides a useful check for the radiometer signal in the analysis.

## Thermocouple Testing Technique

A technique using small thermocouples to measure the temperature rise in compression tests was developed in order to validate the radiometric technique. The method involved embedding a small thermocouple near the surface of the specimen. The ends of the thermocouple were joined to copper wires and placed in two iced-water baths at 0°C for reference. The signal was amplified and recorded using a transient recorder.

The thermocouples used were bare wire K-type and had a diameter of 0.15 mm (Omega Engineering, part CHAL-002). A 0.2 mm hole was drilled in the surface of the cylindrical specimen approximately 1 mm deep. An epoxy resin infiltrated with fine aluminum particles, which will be referred to as Al-epoxy, was used to fix the thermocouple in place (Measurements Group, PC-1 cement). This technique was similar to that used by Dixon[17] in which a 0.7 mm hole was drilled completely through the specimen and soft solder was used to back-fill the hole. The method shown here was less intrusive and would allow a comparison with the radiometry tests.

To interpret the thermocouple results, the response time must be known. The time constant of the thermocouple itself is $\sim$ 45μs. However, the effective response of the thermocouple will be considerably slower, since it is attached to the specimen with Al-epoxy. In this situation, a heat transfer problem must be solved. The finite element package Abaqus was used to simulate the heat transfer from the specimen to the thermocouple. The axisymmetric finite element mesh and boundary conditions are shown in Fig. 3. The thermocouple, Al-epoxy and a small section of the specimen were modeled. Although the thermocouple was very long compared with the scale of the section of the mesh shown, its thermal conductivity was very high compared with the Al-epoxy. For this reason, the whole length of the thermocouple was modeled with a 0°C fixed boundary condition at the end. Because thermal data for the Al-epoxy were unavailable, approximate values were determined experimentally for the specific heat capacity of 1500 $J.kg^{-1}.K^{-1}$ and for the thermal conductivity of 8 $W.m^{-1}.K^{-1}$. The model showed that the time constant for the heating of the thermocouple tip was $\sim$ 900μs, with the temperature reaching 99 percent of its final value in 6 ms.

A typical experimental thermocouple result for a compression test on the aluminum alloy, together with the Abaqus

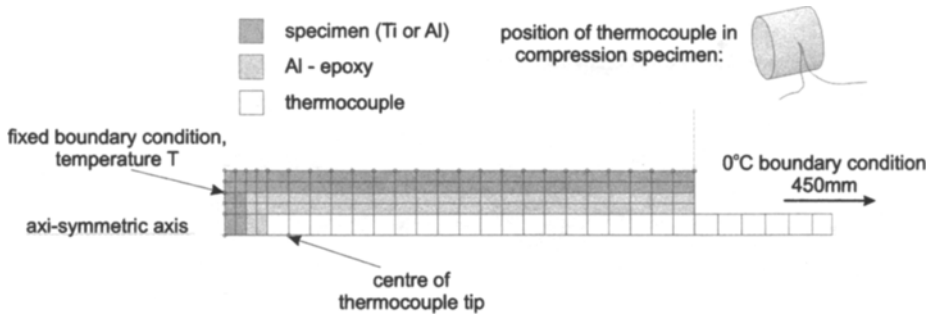


Fig. 3—Finite element mesh for thermocouple heat transfer calculation

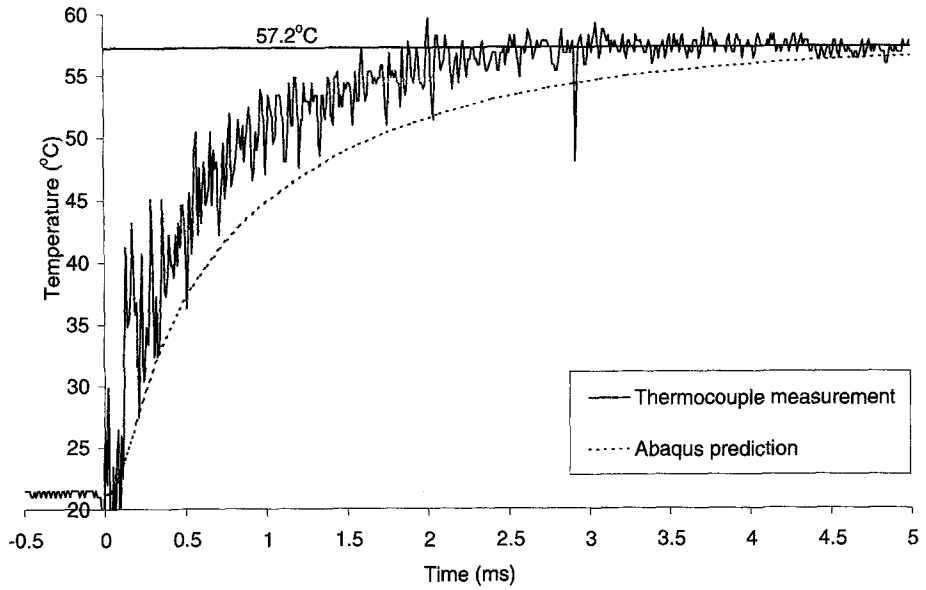


Fig. 4—Temperature rise measured using a thermocouple and predicted using the Abaqus finite element code for a compression test on the aluminum alloy

model result, are shown in Fig. 4. The boundary condition for the model was taken as the final temperature reading made in the test of 57.2°C. The Abaqus model represents the lower bound in terms of the speed of response, in which the thermocouple was glued in the center of the hole with a uniform layer of Al-epoxy surrounding it. All of the experimental results were at least as fast as this model result, often about twice as fast, indicating that the thermocouple was often glued touching the side of the 0.2 mm hole.

Because the thermocouple does not reach equilibrium for about 5 ms to 10 ms, sources of error must be considered. The test lasts approximately 100μs, with the loading bars in contact for a further 100μs. The specimen is then released from the bars and falls for ~ 0.1 s until it strikes the bench. The main source of energy loss is due to conduction during the 200μs in which the specimen is in contact with the loading bars. A simple finite element calculation showed that an average fall in specimen temperature of ~ 0.1°C can be expected as a result of quenching by the loading bars. A simple calculation of the losses by the specimen due to radiation show that this source of error is negligible, with a rate of loss in temperature of ~ $0.07°C.s^{-1}$.

## Results

### *Compression Tests on the Aluminum Alloy BS 2011*

Three compression tests that included radiometry were performed on the aluminum alloy BS 2011. The tests were carried out at a nominally identical strain rate of 2000 $s^{-1}$. The true stress and surface temperature measured in these tests are compared in Fig. 5. The repeatability of the results is quite close, with some spread in the temperature results toward the end of loading. The radiometer signals were analyzed using the calibration shown in Fig. 2. Post-test calibrations were performed on two of the specimens, but no appreciable change in the signal could be found.

To validate the radiometry measurements, compression tests were performed under similar conditions on aluminum alloy specimens with thermocouples embedded near the surface. Because this technique was too slow to follow the specimen temperature during the test, only one measurement was made after the end of loading. To obtain measurements from other points during loading, tests were performed using stop-rings that allow only a predetermined plastic strain in the

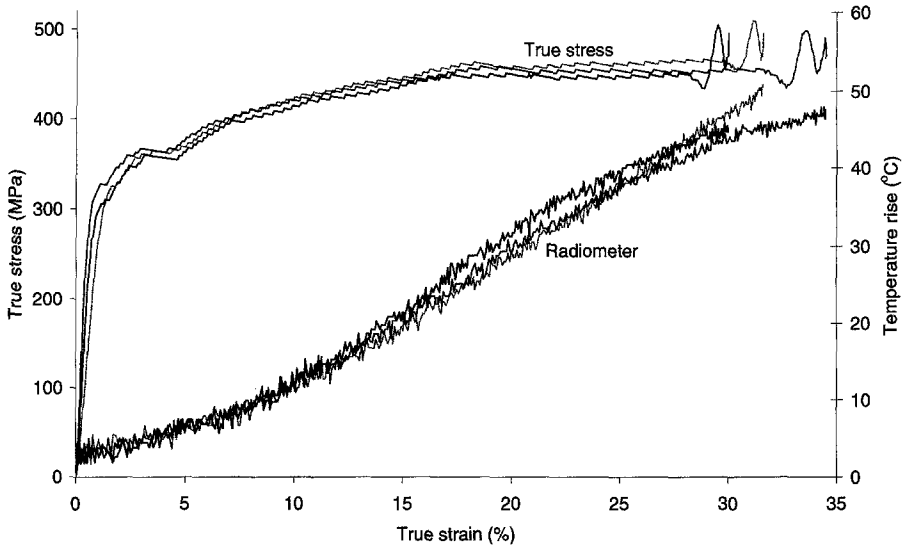


Fig. 5—The true stress and surface temperature for three compression tests on the aluminum alloy

specimen. Two measurements were made at three strains of approximately 12 percent, 23 percent and 32 percent. The thermocouple measurements and average values at each of the strains are shown in Fig. 6. A best-fit line is plotted through the thermocouple results. A linear fit was used for the section between the measurements at 12 percent, 24 percent and 33 percent, and a parabolic fit was used between 0 percent and 12 percent, with the gradients of the two lines matching at 12 percent. Clearly, the choice of this line is not unique.

The average temperature rise for the radiometry tests is shown together with the thermocouple best-fit line in Fig. 7. The radiometer is not accurate below 30°C or for temperature rises of below 8°C, and for this region the average radiometer curve is shown with a dotted line. The radiometer temperature rise is calculated as the difference between the temperature measured using the radiometer and the known temperature measured independently before the test. A best-fit line for the average radiometer curve was constructed in the same way as for the thermocouple results, with an assumption of its form made below the 8°C rise. $\beta$ is calculated as the ratio of the heating rate divided by the plastic work rate. Smooth best-fit lines are necessary to represent the temperature records in order to allow differentiation to produce the heating rate. In Fig. 7, the two best-fit lines are compared with the temperature rise that would be expected if all of the plastic work was converted to heat (corresponding to $\beta = 1.0$). The two best-fit lines fall below this $\beta = 1.0$ line, indicating that the value of $\beta$ for this material is below unity. Also, it should be noted that the gradient of both lines never exceeds that of the $\beta = 1.0$ line.

The value of $\beta$ as it varies with plastic strain is shown in Fig. 8 for both the radiometry and thermocouple measurements. These are compared with the prediction made by the Zehnder model using a value for the strain-hardening constant of $n = 0.5$. The agreement between the model and experiments is good for high strains, but less close for low strains, where assumptions with regard to the shape of the temperature rises were made.

The values of $\beta$ shown in Fig. 8 for the aluminum alloy range from around 0.5 at low strains to around 0.9 at higher strains. The range of values of $\beta$ for aluminum alloys shown in Table 1 is quite varied. However, the general trend of the increase in $\beta$ as plastic strain increases is evident in a number of cases.[5–7,16] The discrepancies between the actual values of $\beta$ measured and the strains at which they occur as compared with the findings of this work could be caused by a number of effects. Errors in the calibration technique for the radiometer, as described earlier, could account for some of the low values of $\beta$ reported in other work. Also, the particular aluminum alloy and its state of prior working could account for the different values of $\beta$ and the plastic strains at which they occur.

### *Torsion Test on the Titanium Alloy 90%Ti-6%Al-4%V*

This was possible because the radiometry apparatus was unchanged and the surface of the torsion specimen was coated in soot in the same manner in the new calibration method. One difference was in the curvature of the specimens. Calculations of the power output per unit area from the two specimens showed that the torsion specimen, with its larger radius of curvature, will produce a smaller radiometer signal by 0.125 percent. The calibration was altered to include this effect. It was not possible to check the change in calibration after the test. In the previous work, the change in calibration was found to be approximately 10 percent. However, the errors in the previous calibration are such that this is of limited reliability, and for this work the calibration was not modified toward the end of the test.

Figure 9 shows the shear stress, the temperature rise calculated using both the new and old calibrations and the expected temperature rise assuming $\beta = 1.0$ for one of the torsion tests. This test was performed at a shear strain rate of 700 $s^{-1}$. It should be noted that the split Hopkinson bar is notoriously poor for calculating elastic strains, and the value of 10 percent strain at yield is not a true measure. The marked difference in the radiometer temperature rises demonstrates the profound effect that the new calibration method had on the previous low-temperature measurements and correspondingly low reported values of $\beta$. Figure 10 shows the calculation of $\beta$ from the test shown in Fig. 9. This is compared with the prediction made by the Zehnder model using a value for the strain-hardening constant of $n = 0.5$. Although the detail

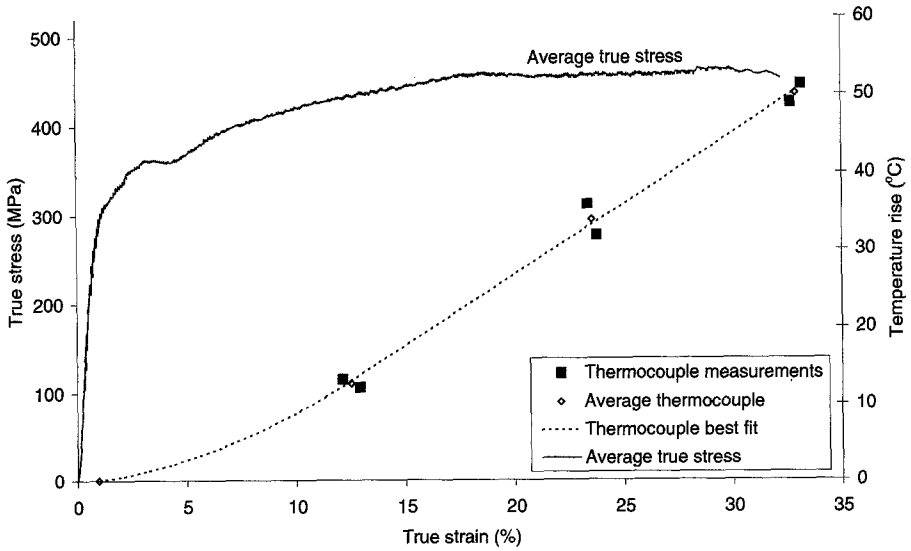


Fig. 6—Average true stress and the temperature measured using thermocouples in six tests on the aluminum alloy

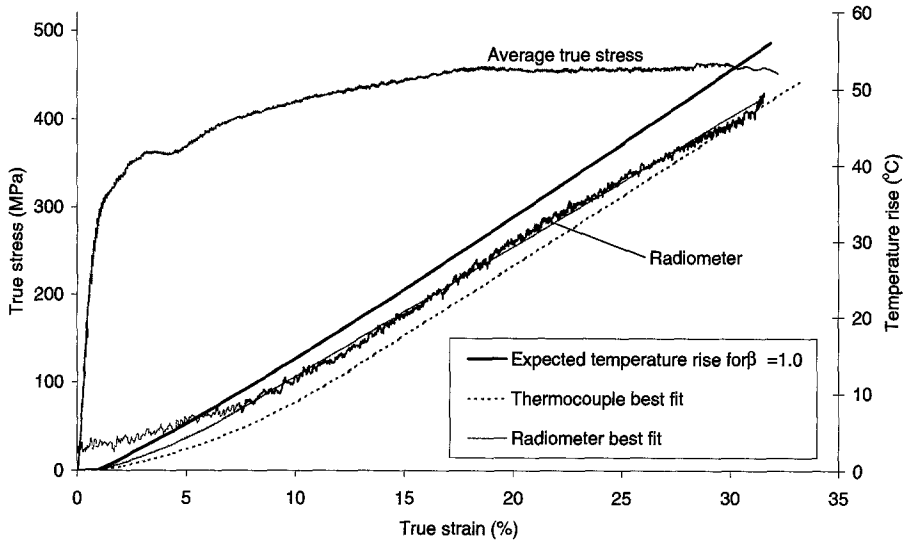


Fig. 7—Average true stress, average surface temperature measured using the radiometer, best-fit lines for temperature rise using the radiometer and thermocouples and the plastic work against true strain for the aluminum alloy

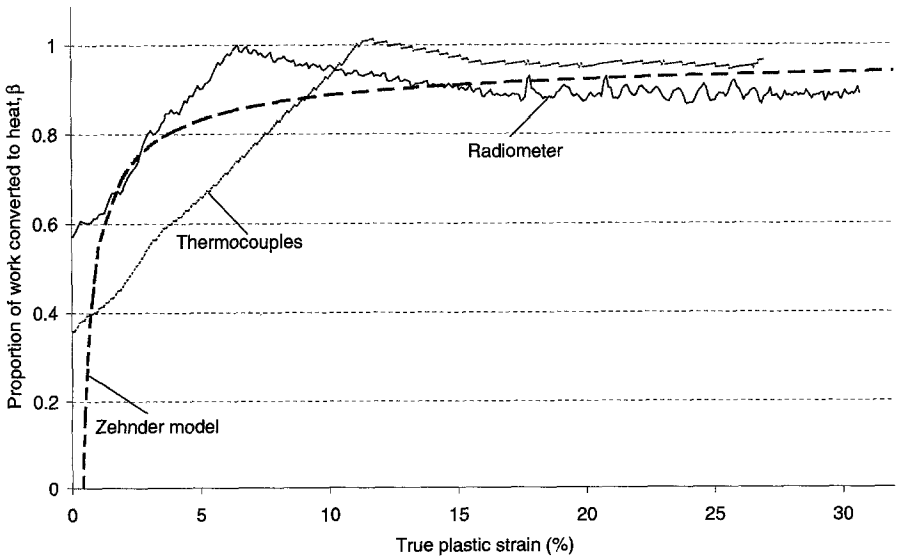


Fig. 8—Proportion of plastic work converted to heat against plastic true strain calculated from both radiometry and thermocouple data and a prediction by the Zehnder model for the aluminum alloy

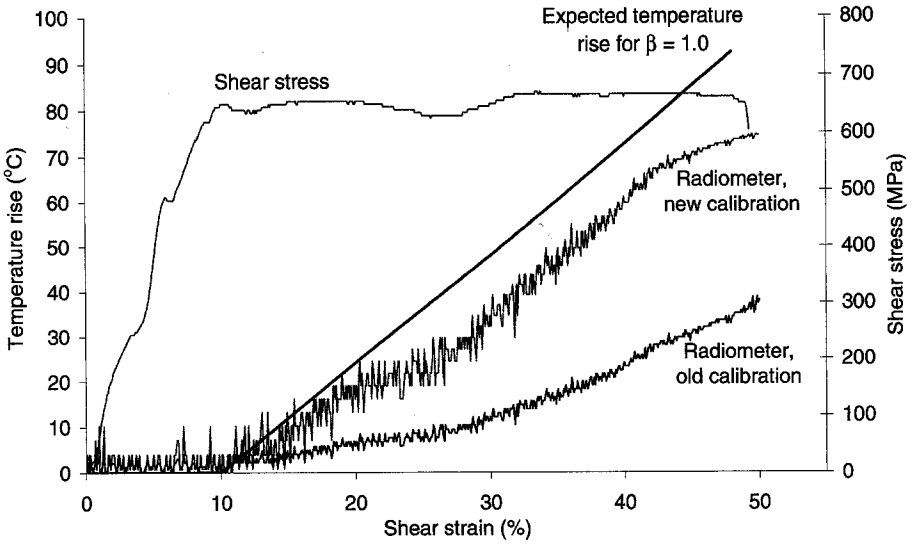


Fig. 9—Shear stress and surface temperature using both the old and new calibrations against shear strain for a torsion test on the titanium alloy

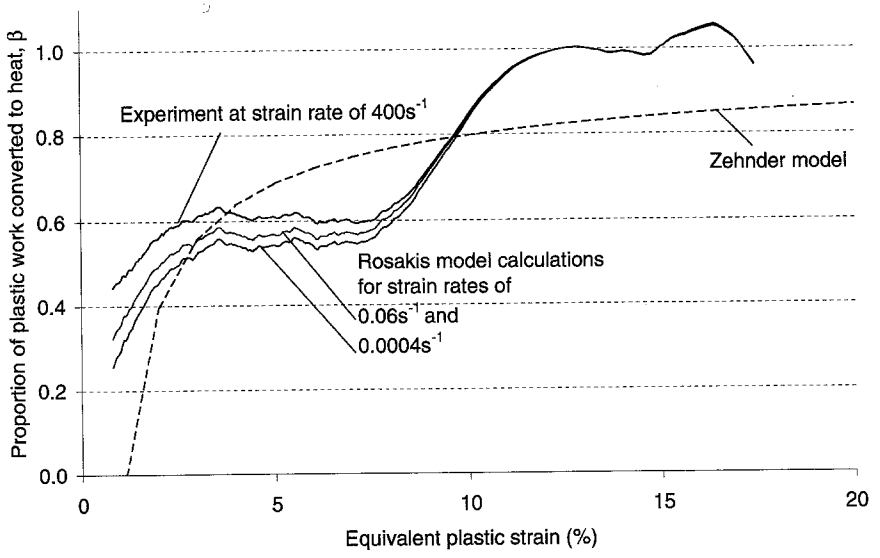


Fig. 10—Proportion of plastic work converted to heat against plastic true strain for the titanium alloy calculated from radiometry data and predictions by both the Zehnder model and the Rosakis model

of the experimental measurement of β is not captured by the model, it agrees with the general trend of β increasing with plastic strain.

The temperature result for the torsion test on the titanium alloy was used to calculate the stored energy of cold work, $E(\varepsilon_p)$, using eq (4). Using torsion stress-strain data for several strain rates for this alloy,[2,3,11] the variation of the proportion of plastic work converted to heat at different strain rates was predicted using Rosakis's model shown in eq (5). Two predictions, based on the result at a strain rate of 400 $s^{-1}$, are shown for strain rates of 0.06 $s^{-1}$ and 0.0004 $s^{-1}$ in Fig. 10. The largest variation for β with strain rate occurs at low strains, where considerable strain hardening is found at quasi-static rates. This titanium alloy shows only moderate strain rate hardening, and therefore the variation of β with strain rate is likely to be much greater for more strain rate sensitive materials.

## Conclusions

A new calibration method was developed for infrared radiometry that simulates the conditions in a high strain rate test more closely than previous calibrations. This is achieved by removing spurious radiation that was present from heated loading bars. Calculations have shown that the radiation from heated air in front of the specimen is negligible.

Compression tests were performed on an aluminum alloy, including temperature measurement using both the radiometric method and small thermocouples. These two techniques have shown good agreement and have validated the new calibration technique. The temperature results were used to calculate the proportion of plastic work that is converted to heat, β. This was found to increase with plastic strain from approximately 0.5 to 0.9, and close agreement was found with a model proposed by Zehnder.

The temperature data from a previous torsion test on a titanium alloy were recalibrated using the new technique, producing substantially higher temperature rises than previously reported.[3] Using the new calibration, $\beta$ was found to increase with plastic strain from approximately 0.5 to 1.0, and fair agreement was found with the Zehnder model. A model by Rosakis was used in conjunction with previous stress-strain data to predict the likely variation of $\beta(\varepsilon_p)$ at different strain rates. Only a small variation of $\beta$ with strain rate was predicted.

The proportion of plastic work that is converted to heat, $\beta$, is an important quantity that is fundamental to temperature calculations by finite element material models involving plasticity. The variation of $\beta$ with strain and strain rate should be investigated further, especially for materials that exhibit considerable strain hardening and strain rate sensitivity.

## References


*1. Macdougall, D. and Harding, J., "The Measurement of Specimen Surface Temperature in High-speed Tension and Torsion Tests," Int. J. Impact Eng.*, **21**, *473–488 (1998).*

*2. Macdougall, D. and Harding, J., "Materials Testing for Constitutive Relations," J. de Physique III, suppl. C3, 103–108 (1997).*

*3. Macdougall, D. and Harding, J., "A Constitutive Relation and Failure Criterion for Ti6Al4V Alloy at Impact Rates of Strain," J. Mech. Phys. Solids*, **47**, *1157–1185 (1999).*

*4. Trojanowski, A., Macdougall, D., and Harding, J., "An Improved Technique for the Experimental Measurement of Specimen Surface Temperature During Hopkinson Bar Tests," Meas. Sci. Tech.*, **9**, *12–19 (1998).*

*5. Hayashi, T., Yamamura, H., and Okano, S., "Temperature Measurement of Metals Under High Velocity Deformation," Society of Materials Science, Kyoto, 94–98 (1977).*

*6. Mason, J.J., Rosakis, A.J., and Ravichandran, G., "On the Strain and Strain Rate Dependence of the Fraction of Plastic Work Converted to Heat: An Experimental Study Using High Speed Infrared Detectors and the Kolsky Bar," Mech. Mat.*, **17**, *135–145 (1994).*

*7. Xia, Y., Rao, S., and Yang, B., "An Infrared Transient Temperature Measuring Apparatus and Its Application to the Tensile Impact Testing," Exp. Mech.*, **5**, *170–176 (1990) (in Chinese).*

*8. Kapoor, R. and Nemat-Nasser, S., "Determination of Temperature Rise During High Strain Rate Deformation," Mech. Mat.*, **27**, *1–12 (1998).*

*9. Zehnder, A.T. and Rosakis, A.J., "On the Temperature Distribution at the Vicinity of Dynamically Propagating Cracks in 4340 Steel," J. Mech. Phys. Solids*, **39**, *385–415 (1991).*

*10. Hartley, K.A., Duffy, J., Hawley, R.H., "Measurement of the Temperature Profile During Shear Band Formation in Steels Deforming at High Strain Rates," J. Mech. Phys. Solids*, **35**, *283–301 (1987).*

*11. Macdougall, D.A.S., "Materials Testing for Constitutive Relations," Doctoral thesis, Christ Church, Oxford University (1997).*

*12. Trojanowski, A., Ruiz, C., and Harding, J., "Thermomechanical Properties of Polymers at High Rates of Strain," J. de Physique III, suppl. C3, 447–452 (1997).*

*13. Chrysochoos, A., Maisonneuve, O., Martin, G., Caumon, H., and Chezeaux, J.C., "Plastic and Dissipated Work and Stored Energy," Nucl. Ener. Des.*, **114**, *323–333 (1989).*

*14. Rittel, D., "On the Conversion of Plastic Work to Heat During High Strain Rate Deformation of Glassy Polymers," Technical Report No. TME 459, Technion–Israel Institute of Technology (Feb. 1998).*

*15. Taylor, G.I. and Quinney, H., "The Latent Energy Remaining in a Metal After Cold Working," Proc. Roy. Soc. A*, **143**, *307–326 (1933).*

*16. Hodowany, J., Ravichandran, G., Rosakis, A.J., and Rosakis, P., "On the Partition of Plastic Work into Heat and Stored Energy in Metals: Part I. Experiments," Internal SM Report No. 98-7, California Institute of Technology (June 1998).*

*17. Dixon, P.R. and Parry, D.J., "Thermal Softening Effects in Type 224 Carbon Steel," J. de Physique III, suppl. C3, 85–92 (1991).*

*18. Zehnder, A.T., "A Model for the Heating Due to Plastic Work," Mech. Res. Comm.*, **18**, *23–28 (1991)..*

*19. Rosakis, P., Rosakis, A.J., Ravichandran, G., and Hodowany, J., "On the Partition of Plastic Work into Heat and Stored Energy in Metals: Part II. Theory," Internal SM Report No. 98-8, California Institute of Technology (June 1998).*

*20. MODRAN Version 3.7, U.S. Air Force.*

*21. Rittel, D., "Transient Temperature Measurement Using Embedded Thermocouples,"* EXPERIMENTAL MECHANICS, **38**, *73–78 (1998).*